Eur. Phys. J. C (2021) 81:569
https://doi.org/10.1140/epjc/s10052-021-09353-9

THE EUROPEAN PHYSICAL JOURNAL C

Regular Article - Theoretical Physics

Quark star matter at finite temperature in a quasiparticle model

Peng-Cheng Chu[1,a], **Yao-Yao Jiang**[1,b], **He Liu**[1,2,c], **Zhen Zhang**[3,d], **Xiao-Min Zhang**[1,2,e], **Xiao-Hua Li**[4,5,f]

[1] The Research Center for Theoretical Physics, Science School, Qingdao University of Technology, Qingdao 266033, China
[2] The Research Center for Theoretical Physics, Qingdao University of Technology, Qingdao 266033, China
[3] Sino-French Institute of Nuclear Engineering and Technology, Sun Yat-sen University, Zhuhai 519082, China
[4] School of Nuclear Science and Technology, University of South China, Hengyang 421001, China
[5] Cooperative Innovation Center for Nuclear Fuel Cycle Technology and Equipment, University of South China, Hengyang 421001, China

Received: 10 February 2021 / Accepted: 19 June 2021

Abstract We study the thermodynamic properties of asymmetric quark matter, large mass quark stars (QSs), and proto-quark stars (PQSs) within the quasiparticle model. Considering the effects of temperature within quasiparticle model can significantly influence the EOS and the entropy of strange quark matter (SQM), quark fractions in SQM, as well as the tidal deformability and the maximum mass of PQSs along the star evolution line. Our results indicate that the recent discovered heavy compact stars PSR J0348+0432, MSR J0740+6620, PSR J2215+5135, and especially the GW190814's secondary component m_2 can be well described as QSs within the quasiparticle model. The tidal deformability for the QSs describing the heavy compact stars is extremely large, which can not well describe GW170817 as QSs, and the effects of the temperature in the heating process along the star evolution will further increase the tidal deformability and the maximum mass of PQSs.

1 Introduction

As one of the fundamental issues in modern nuclear physics, cosmology, and astrophysics [1–4], the investigation of the properties of strongly interacting matter plays a central role in discovering the nuclear structures and reactions and the matter state at early universe. The study of composition of the matter in the deep dense interior of neutron stars (NSs) has been lasted for over eight decades, and strange component like hyperons, kaons, or even deconfined quark matter phase formed from the melted baryons are supposed to appear in the dense matter inside NSs. At present, one of the hot topics in compact object studies is the appearance of quark matter in massive neutron stars (NSs). Strange quark stars (QSs), whose possible existence is still considered as the most important fields of astrophysics and nuclear physics [5–11], could be theoretically converted from NSs, and this hypothesis cannot be conclusively ruled out. QSs usually has large u-d quark asymmetry and can be totally made up of deconfined strange quark matter (SQM), including the absolutely stable u, d and s quarks with leptons in β-equilibrium condition [7,8,12–16].

A proto-neutron star (PNS) usually forms after the gravitational collapse in the core of massive star with the explosion of a supernova. The formation of PNSs was well studied in the work [17], while people still know little about the transition from PNS to proto-quark stars (PQS) during the type II supernova explosion owing to complexity of the burning process from hadron matter to SQM. From the results in the work [10,18–24], PQSs could be produced from the neutron stars merging, and there might be a dynamically unimportant crust of nucleonic matter with densities below the neutron drip density for PQS.

In recent reports of the precise measurements of heavy pulsars, a heavy pulsar PSR J0348+0432 with a mass of $2.01 \pm 0.04\ M_\odot$ [25] was discovered in 2013, while a more massive compact star PSR J 2215+5135, whose star mass reaches $2.27^{+0.17}_{-0.15}\ M_\odot$ [26], has been detected by fitting the radial velocity lines and the three-band light curves in the irradiated compact stars model. In Ref. [27], the MSR J0740+6620 ($2.14 \pm^{0.10}_{0.09} M_\odot$ with 68.3% credibility interval and $2.14 \pm^{0.20}_{0.18} M_\odot$ with 95.4% credibility interval) is reported as the most massive precisely observed pulsar by using the data of relativistic Shapiro delay with the Green Bank Telescope. These observations of supermassive compact star can set strict constraints on the equation of state

[a] e-mail: kyois@126.com (corresponding author)
[b] e-mail: Jiangyaoyao_yy@163.com
[c] e-mail: liuhe@qut.edu.cn
[d] e-mail: zhangzh275@mail.sysu.edu.cn
[e] e-mail: zhangxm@mail.bnu.edu.cn
[f] e-mail: lixiaohuaphysics@126.com

Published online: 01 July 2021

(EOS) of star matter and rule out most of the conventional phenomenological models for quarks, while there still exist some other models which can provide heavy quark stars with strong isospin interaction inside the star matter [28–37]. In particular, the newly discovered compact binary merger GW190814 [38] from the LIGO/Virgo Collaborations involving a 22.2−22.3 $M_\odot$ black hole and a compact object, which includes a secondary component m_2 with the mass of 2.50 $M_\odot$−2.67 $M_\odot$ at 90% credible level, has attracted extensive attention in modern physics society. The candidate for the secondary component of GW190814 could be compact stars or light black hole, which can put very strict constraints on the EOS of nuclear matter because of the extremely large star mass. On the other hand, LIGO-Virgo collaboration [39] detected the gravitational wave (GW) signal GW170817 event from a binary compact star system three years ago, and lots of works on the constraints on the thermodynamic properties of the star matter have been calculated based on this observation [40–49]. The LIGO-Virgo collaboration investigates the tidal deformability of the compact objects and proposes an upper limit of $\Lambda_{1.4} < 800$ for the low-spin priors of the 1.4 solar mass pulsars in Ref. [39], and then the constraints on the properties of the nuclear matter symmetry energy and the EOS of strongly interacting matter have been calculated from many works based on the upper limit for the tidal deformability [42,46,47,50–56]. Furthermore, in Refs. [45,57,58], GW170817 can also have the possibility to be produced from the binary quark/hybrid star merger, where the limitations of $\tilde{\Lambda}$ at 1.4 $M_\odot$ was constrained as (0, 630) for large spin pulsar, 300^{+420}_{-230} for the largest posterior density interval, and $\Lambda_{1.4} = 190^{+390}_{-120}$ by using the Λm^5 linear expansion in the works [38,42,59,60].

In the present work, we investigate the properties of the equation of state of strange quark matter (SQM), the quark fraction, the entropy per baryon of SQM, the maximum mass of QSs and PQSs, as well as the tidal deformability for QSs by using the quark quasiparticle model. We find that the recent discovered supermassive compact stars can be well described as QSs within quasiparticle model, and the heating process along the star evolution line can increase the maximum mass of PQSs within quasiparticle model.

2 Models and methods

2.1 The quasiparticle model

Using the hard dense loop approximation [61], the effective quark mass of the quasiparticle model was derived at the zero-momentum limit of the dispersion relations by resuming one-loop self energy diagrams, which is defined differently from the conventional density-dependent quark mass model, whose effective quark mass includes only the density-dependent quark–quark effective interactions [61–93]. The effective quark mass for each flavor of quarks within quas4iparticle model can be expressed as [61,94–96]

$$m_q = \frac{m_{q0}}{2} + \sqrt{\frac{m_{q0}^2}{4} + \frac{g^2\mu_q^2}{6\pi^2}}, \tag{1}$$

where m_{q0} is the current mass for quarks, which is set as $m_{u0} = 5.5$ MeV, $m_{d0} = 5.5$ MeV, and $m_{s0} = 95$ MeV respectively in this work. μ_q means the chemical potential for the ith flavor of quarks, and g represents the coupling constant of the strong interaction which is considered as one free input parameter in this work. In the previous works [61,94–96], the authors study the thermodynamical properties of asymmetric quark matter at zero temperature or under strong magnetic fields by using quasiparticle model. From their work, the thermodynamical self-consistency of the quasiparticle model has been checked, but the EOS of the star matter is not stiff and cannot describe heavy compact stars (at least 2 solar mass QSs) as QSs. In this work, we first calculate the thermodynamical properties of SQM at finite temperature, and then discuss the tidal deformability and the maximum mass (larger than 2 solar mass) of PQSs along the star evolution line by using quasiparticle model.

The total thermodynamic potential density for SQM can then be written as

$$\Omega = \sum_i [\Omega_i + B_i(\mu_i)] + B, \tag{2}$$

where Ω_i in the sum shows the contribution to the thermodynamic potential density for quarks (u, d, and s) and leptons (e and μ), $B_i(\mu_i)$ is the additional medium dependent terms determined by thermodynamical self-consistency, and B is considered as the negative vacuum pressure term for nonperturbative confinement [97]. The expression of Ω_i for quarks and leptons at finite temperature is written as

$$\Omega_i = -\frac{g_i T}{2\pi^2}\int_0^\infty \left[\ln\left(1+\mathrm{e}^{-(\sqrt{p^2+m_i^2}-\mu_i)/T}\right) + \ln(1+\mathrm{e}^{-(\sqrt{p^2+m_i^2}+\mu_i)/T}\right] p^2 \mathrm{d}p, \tag{3}$$

where g_i is the degeneracy factor with $g_i = 2$ for leptons and $g_i = 6$ for quarks. The medium dependent term $B_i(\mu_i)$ is determined as

$$B_i(\mu_i) = -\int_0^\infty \frac{\partial\Omega_i}{\partial m_i}\frac{\partial m_i}{\partial \mu_i}\mathrm{d}\mu_i. \tag{4}$$

2.2 Properties of strange quark matter at finite temperature

Strange quark matter is assumed to be composed of quarks (u, d, and s) and leptons (e and μ) and satisfies the electric charge neutrality in beta-equilibrium. The beta-equilibrium

condition at finite temperature can be expressed as

$$\mu_d = \mu_s = \mu_u + \mu_e - \mu_{\nu_e},$$
$$\mu_\mu = \mu_e, \quad \text{and} \quad \mu_{\nu_\mu} = \mu_{\nu_e}. \tag{5}$$

The electric charge neutrality condition can be written as

$$\frac{2}{3}n_u = \frac{1}{3}n_d + \frac{1}{3}n_s + n_e + n_\mu, \tag{6}$$

where the number density for the particle with flavor i can be obtained as

$$n_i = \frac{g_i}{2\pi^2}\int_0^\infty \left[\frac{1}{1+e^{(\epsilon_i-\mu_i)/T}} - \frac{1}{1+e^{(\epsilon_i+\mu_i)/T}}\right] p^2 \mathrm{d}p. \tag{7}$$

Here $\epsilon_i = \sqrt{p^2+m_i^2}$ is the energy dispersion for particles. The total free energy density $\mathcal{F}$ and the pressure P are, respectively, written as

$$\mathcal{F} = \sum_i \mathcal{F}_i = \sum_i (\Omega_i + B_i(\mu_i) + \mu_i n_i) + B, \tag{8}$$

$$P = -\sum_i (\Omega_i + B_i(\mu_i)) - B. \tag{9}$$

And the total energy density can be written as $\mathcal{E} = \sum_i \mathcal{E}_i$ with

$$\mathcal{E}_i = \frac{g_i}{2\pi^2}\int_0^\infty \left[\frac{\epsilon_i}{1+e^{(\epsilon_i-\mu_i)/T}} + \frac{\epsilon_i}{1+e^{(\epsilon_i+\mu_i)/T}}\right] p^2 \mathrm{d}p. \tag{10}$$

Then the entropy density relevant to Ω_i in the preceding equations can be calculated as

$$S = \sum_i S_i = -\sum_i \frac{\partial \Omega_i}{\partial T}. \tag{11}$$

Considering $\mathcal{F}_i = \mathcal{E}_i - TS_i$, one can obtain the thermodynamical self-consistency by solving Eqs. (8), (10) and (11).

3 Results and discussions

3.1 Equation of state at finite temperature

The absolute stability of SQM/udQM has been proposed in the work [9], which means that the minimum value of the energy per baryon of SQM/udQM at zero temperature should be less/larger than 930 MeV (the minimum binding energy per baryon of the observed stable nuclei $M(^{56}Fe)/56$) at zero temperature, and the absolutely stable condition usually sets very strict constraints on the parameter chosen space for lots of the phenomenological quark mass models. In Fig. 1, we calculate the free energy per baryon and the energy per baryon for SQM as functions of the baryon number density within the quasiparticle model with different parameter sets at the temperature of 0, 30 MeV, and 50 MeV. Considering the absolute stability for quark matter, the parameters are set as g-2 ($g = 2$, $B^{1/4} = 141$ MeV), g-3 ($g = 3$, $B^{1/4} = 136$ MeV), g-4 ($g = 4$, $B^{1/4} = 131$ MeV), and g-5 ($g = 5$, $B^{1/4} = 120$ MeV), which can satisfy the absolute stability for SQM and udQM at zero temperature with the quasiparticle model. From the figure we can find that the energy per baryon increases with the temperature at a certain baryon density, while the free energy per baryon decreases with the temperature. The split between $\mathcal{F}$ and $\mathcal{E}$ is expected to be due to the effect of temperature in the equation $\mathcal{F} = \mathcal{E} - TS$. Furthermore one can see that the minimum value of the free energy per baryon/energy per baryon decreases/increases with the increment of the coupling constant g, and the corresponding baryon density of the minimum value of the free energy per baryon decreases with both the temperature and g.

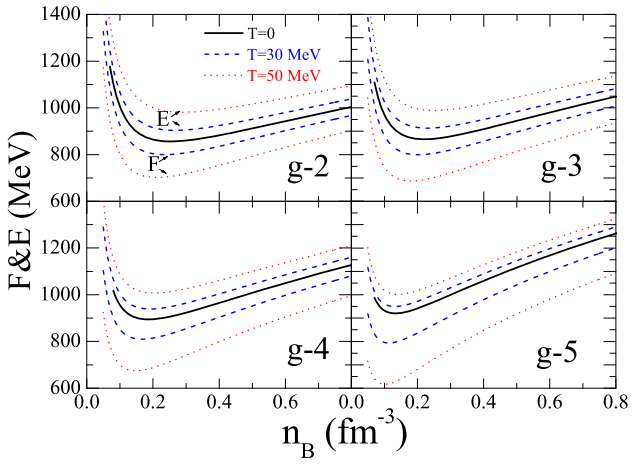

Fig. 1 Free energy per baryon and energy per baryon as functions of the baryon density for SQM within the quasiparticle model with different parameter sets at finite temperature

Figure 2 shows the pressure of SQM as a function of the baryon number density with different sets of parameters at $T = 0$, $T = 30$ and 50 MeV. We can find for all the four cases, the baryon density of the zero-pressure point in Fig. 2 is exactly the baryon density of the minimum value of the corresponding free energy per baryon in Fig. 1, which satisfies the thermodynamical self-consistency of the quark matter. Furthermore, we can see that the baryon density of the zero-pressure point decreases with both temperature and g. In particular, one can also find the pressure of SQM increases with both the temperature and g, which indicates that the effects of the temperature of SQM and the coupling constant g can both stiffen the EOS of SQM to support heavy QSs.

In Fig. 3, we calculate the quark fractions of u, d and s quarks in SQM with different sets of parameters at $T = 0$ and 50 MeV. One can see that the d quark fraction is larger than u

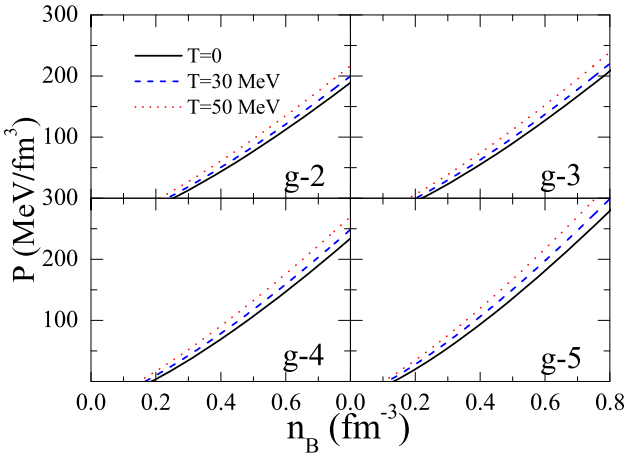

Fig. 2 Pressure as a function of baryon density in different temperature cases

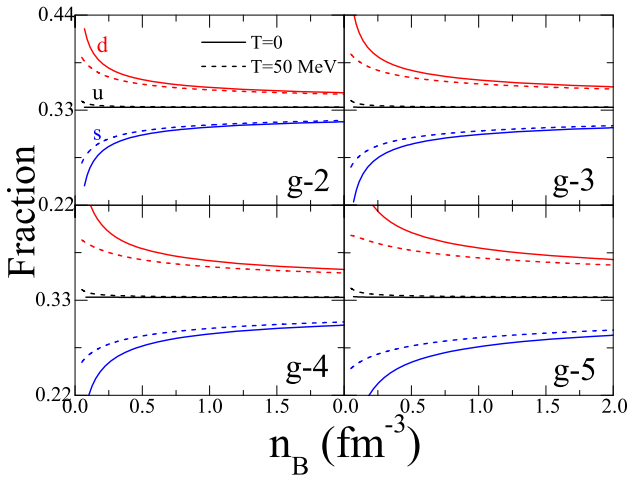

Fig. 3 Quark fractions as functions of the baryon density in SQM with g-2, g-3, g-4, and g-5 in different temperature cases

and s quark fractions at low baryon density for all the cases, and the difference among u, d, and s quark fraction decreases with the baryon density for the four cases at both $T = 0$ and 50 MeV. One can also find that the difference of the quark fractions decreases when the temperature increasing, which implies that the u, d, and s quark fraction can almost be identical at low baryon density region when temperature increases large enough.

Figure 4 shows the entropy per baryon of SQM as a function of the baryon density with g-2, g-3, g-4, and g-5 at $T = 30$ and 50 MeV. One can see in Fig. 4 that the entropy per baryon of SQM decreases with the baryon density for all cases, and the entropy per baryon increases when the temperature increases from 30 MeV to 50 MeV at a certain g, which indicates the degree of disorder for SQM increases at high temperature. We can also find that the entropy per baryon increases with the coupling constant g at a fixed temperature, which is consistent with the increasing split between the free

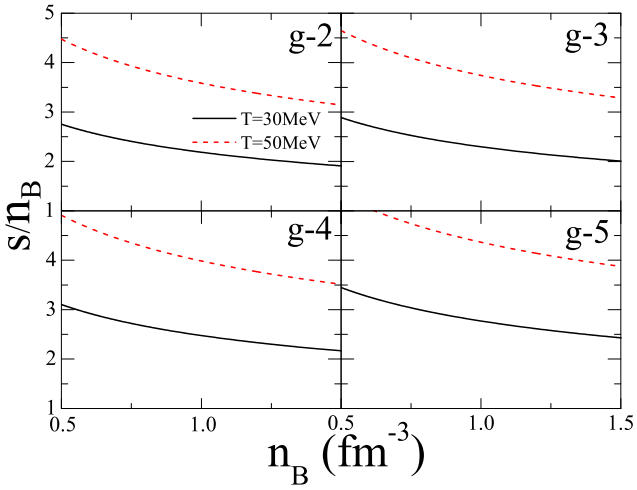

Fig. 4 Entropy per baryon for SQM as a function of the baryon density with g-2, g-3, g-4, and g-5 in different temperature cases

energy per baryon and the energy per baryon causing by the increasing g in Fig. 1. These results indicate that considering the temperature effects inside the SQM and increasing the coupling constant g in the quasiparticle model can both stiffen the EOS of SQM and increase the entropy per baryon of the strongly interacting matter, which can support heavy QSs and increase the complexity of the system.

3.2 Properties of proto-quark stars

One can then calculate the Mass-radius relation of static QSs by solving the Tolman–Oppenheimer–Volkoff (TOV) equation [98]:

$$\frac{dM}{dr} = 4\pi r^2 \epsilon(r), \tag{12}$$

$$\frac{dp}{dr} = -\frac{G\epsilon(r)M(r)}{r^2}\left[1+\frac{p(r)}{\epsilon(r)}\right] \times \left[1+\frac{4\pi p(r) r^3}{M(r)}\right]\left[1-\frac{2GM(r)}{r}\right]^{-1}, \tag{13}$$

where $M(r)$ is the total mass inside the sphere of radius r, G is Newton's gravitational constant, and $\epsilon(r)$ and $p(r)$ are the corresponding energy density and the pressure for quark star matter. The TOV equations of QSs is solved by integrating the equations from the central density to the surface baryon density (which is just the zero-pressure density), because QSs have no crust.

In this work, we describe the time evolution of PQS in its first minutes of life by three snapshots as

$$\text{(I) } S/n_B = 1, Y_l = 0.4, \tag{14}$$

$$\text{(II) } S/n_B = 2, Y_{\nu_l} = 0, \tag{15}$$

$$\text{(III) } S/n_B = 0, Y_{\nu_l} = 0, \tag{16}$$

which follows the way of the previous studies [17,21,99–103] to describe the evolution of PQS as that of PNS. At the first snapshot of PQS evolution after the gravitational collapse with the explosion of a supernova, the entropy per baryon is set about one and the number of leptons per baryon with trapped neutrinos is about 0.4 ($Y_l = Y_e + Y_\mu + Y_{\nu_l} = Y_e + Y_\mu + Y_{\nu_e} + Y_{\nu_\mu} = 0.4$). In the following tens of seconds, the diffusing neutrinos heat the star matter and escape from the star, which could increase the corresponding entropy density, and then the decreasing neutrino fraction reaches almost zero while the entropy per baryon increasing to 2. Following the heating stage, the star starts cooling with the neutrino pairs radiating, and then finally the conventional cold quark star forms. In this work, we do not study the evolution of an isolated star with the baryon number density being fixed.

In Fig. 5, we calculate the mass-radius relation of QSs with g-2, g-3, g-4, and g-5 at zero temperature case, and the three snapshots along the PQS evolution for g-4 and g-5 are also included. For comparison, we also added the large compact star mass value $2.59^{+0.08}_{-0.09} M_\odot$ (90% CL) from GW190814 [38] and two independent constraints of the simultaneous M-R measurements from NICER (through the analysis of the X-ray data for the millisecond pulsar PSRJ0030+451) [104,105]. It can be seen from Fig. 5 that the results of the maximum mass of QSs with g-2 can describe the PSR J0348+0432 with the mass of $2.01 \pm 0.04 M_\odot$ [25] as QSs, while it cannot satisfy the constraint from NICER because of the small radius of QSs. Furthermore, the results of the maximum mass of QSs with g-3, g-4, and g-5 are all consistent with the constraints from NICER, and one can describe the recently discovered massive pulsar MSR J0740+6620 ($2.14 \pm^{0.10}_{0.09} M_\odot$ of 68.3% credibility interval and $2.14 \pm^{0.20}_{0.18} M_\odot$ of 95.4% credibility interval) [27] and PSR J2215+5135 with the mass of $2.27 \pm^{0.10}_{0.09} M_\odot$ as QSs with g-3 and g-4, respectively. For the case g-5, the result shows that the maximum mass of the QS is $2.59 M_\odot$, which is able to describe the GW190814's secondary component as QSs within quasiparticle model.

For the PQS cases of g-4 and g-5, the maximum mass of PQS with g-4 (g-5) is 2.30 $M_\odot$ (2.63 $M_\odot$) and 2.33 $M_\odot$ (2.67 $M_\odot$) for stage I and stage II, respectively, which implies that the star mass of PQSs is larger during the heating stages of stage I and stage II. Furthermore, we can obtain that the largest star mass of the three snapshots along the star evolution can be found at $S/n_B = 2$ stage for both g-4 and g-5 cases within quasiparticle model. Then our results indicate that we can describe the secondary component of GW190814 as QSs at $S = 0$ stage along the star evolution line, and the maximum mass of stars at the heating process stages usually becomes larger when PQSs forms, which indicates the effects of temperature can stiffen the EOS of the star matter and support more massive stars.

The thermodynamic properties of the star matter can also be concluded by using the observation of tidal effects in binary compact star system, because the tidal deformation can be determined by the internal structure of the compact stars. In Table 1, we list the maximum mass and the tidal deformability $\Lambda_{1.4}$ of QSs and PQSs with g-2, g-3, g-4 and g-5, and one can find that only $\Lambda_{1.4}$ for g-2 in S=0 case can satisfy the upper limit $\Lambda_{1.4} < 800$ derived from GW170817, while the cases of the heavier stars (g-3, g-4, and g-5) all strongly violates the constraint $\Lambda_{1.4} < 800$ derived from GW170817. One can also see that the tidal deformability $\Lambda_{1.4}$ increases with the coupling constant g within quasiparticle model (especially the tidal deformability $\Lambda_{1.4}$ even larger than 2000 for g-5). Since the tidal deformability of 1.4 solar mass for the QS whose maximum mass is 2.59 solar mass (candidate of GW190814) within quasiparticle model is far beyond the upper bound of 800 found by LIGO, we should point out that our results within quasiparticle model is not acceptable for describing GW170817 as QSs unless we choose the maximum star mass with the parameterization of the quasiparticle model is less than 2.14 solar mass (when $\Lambda_{1.4} < 800$). As we have mentioned in Fig. 5 that the results of g-5 can be in agreement with NICER radius measurements with $\Lambda_{1.4} > 2000$, which is very large and seems to be mismatched. The reason for this phenomenon why the result of that large tidal deformability can still satisfy the NICER results is complicated, and one can find in Eq. (2) to Eq. (4) of Ref. [106] that the computation of tidal love numbers and the tidal deformability are dependent on the star mass, star radius, the EOS of star matter (conventionally during the calculation of the maximum mass and radius for QSs, people stop the TOV integrations at zero pressure point, which is of great importance for the determination of stellar mass and different from the criteria used for stopping the TOV integrations for NSs), the squared sound speed, the central density of the star, etc. In the left panel of Fig. 6, we show

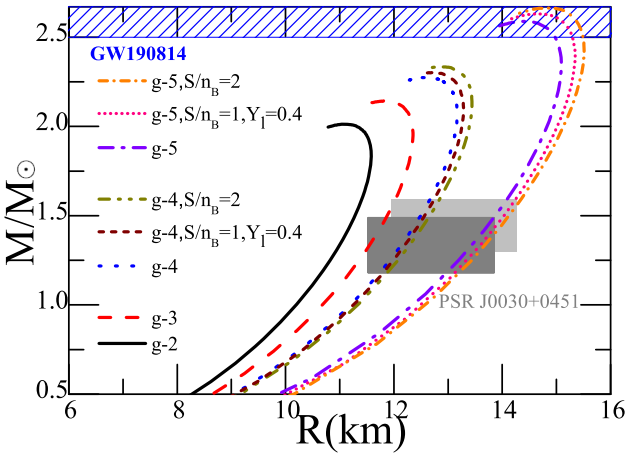

Fig. 5 Mass-radius relation with g-2, g-3, g-4, and g-5 at zero temperature and the three snapshots along the PQS evolution for g-4 and g-5 are also included

Table 1 The maximum mass and the corresponding tidal deformability $\Lambda_{1.4}$ of QSs and PQSs within quasiparticle model with g-2, g-3, g-4, and g-5

Parameter sets	g-2	g-3	g-4	g-5
$M(M_\odot, S=0)$	2.01	2.14	2.27	2.59
$M(M_\odot, S/n_B=1, Y_l=0.4)$	2.03	2.16	2.30	2.63
$M(M_\odot, S/n_B=2)$	2.05	2.18	2.33	2.67
$\Lambda_{1.4}, S=0$	588	826	1150	2236
$\Lambda_{1.4}, S/n_B=1, Y_l=0.4$	602	843	1189	2438
$\Lambda_{1.4}, S/n_B=2$	615	857	1245	2550

the mass-radius relation of QSs for g-5 within quasiparticle model and the mass-radius relation of NSs within MDI interaction [107] (in this work, we set $x=-1$, $K_0=230$ MeV, $E_{sym}(\rho_0)=32.5$ MeV, and $E_0(\rho_0)=-16$ MeV for the MDI interaction, and the maximum mass of NS for this case is 2.16 solar mass), and one can see that both the radius for the two cases at the mass of 1.4 $M_\odot$ for compact stars are exactly 13.6 km and satisfy the radius measurements of NICER. From the results, the central density of the 1.4 solar mass at the same radius for QS and NS are different, which are 0.19 and 0.37 fm^{-3}, respectively. For the right panel of Fig. 6, one can find that the pressure of the two cases for the star matter is totally different (the pressure of quark star matter is much larger than that of the neutron star matter), which can make different contributions to the tidal love number and the tidal deformability. As we have already shown in Table 1, $\Lambda_{1.4}$ of g-5 is 2236 at zero temperature with the radius being 13.6 km, while the tidal deformability $\Lambda_{1.4}$ for neutron star with MDI interaction at the same radius is only 771, which indicates that the value of the tidal deformability of the compact stars is very complicated and depends on not only the star mass and radius but also the EOS and other physical quantities of the star matter. Additionally, in the recent work from Cao [108], their results in Fig. 1 also show that the tidal deformability could be extremely large once heavy QSs is calculated by using ICQM model with a very stiff EOS, which satisfies the NICER measurement too. Therefore, the results imply that large QSs within some phenomenological models might satisfy the NICER radius result with large tidal deformability. Furthermore, we can obtain in Table 1 that the tidal deformability $\Lambda_{1.4}$ for PQSs is larger in the heating stages for different sets of parameters, and the largest $\Lambda_{1.4}$ appears in the 2nd stage of the three snapshots along the star evolution for both cases.

In Fig. 7, we calculate the core temperature of QSs as a function of the baryon density with g-4 and g-5 for Stage I and II. The central density for the maximum mass of QSs with g-4 for stage I (II) is 0.73 fm^{-3} (0.71 fm^{-3}), while the central density for the maximum mass of QSs with g-5 for stage I (II) is 0.55 fm^{-3} (0.53 fm^{-3}), which implies that the central density for the maximum mass of QSs decreases with the entropy per baryon of the stages along the star evolution line. One can also find the corresponding core temperature of PQSs T_c at different stages increases from 9.7 MeV to 21.4 MeV with g-4, while T_c increases from 7.8 MeV to 17.1 MeV with g-5, which implies that the core temperature of PQSs increases with the entropy per baryon of the stages along the star evolution line (this result is consistent with the conclusion that the entropy per baryon for SQM increases with the temperature). In particular, we can obtain that the core temperature of PQSs at the certain stage of the star evolution line decreases with the increment of the coupling constant g.

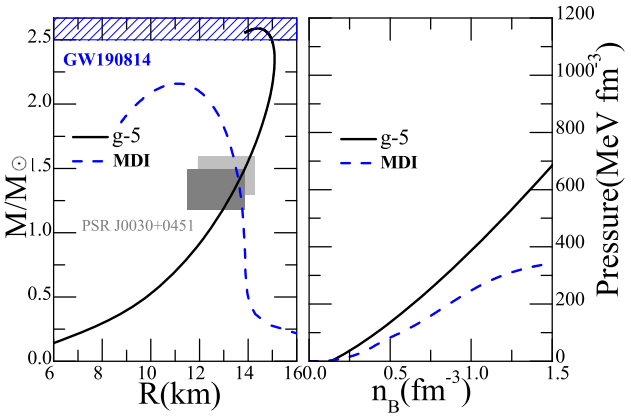

Fig. 6 Left panel: Mass-radius relation for quark stars and neutron stars. Right panel: The pressure of quark star matter and neutron star matter as functions of baryon density

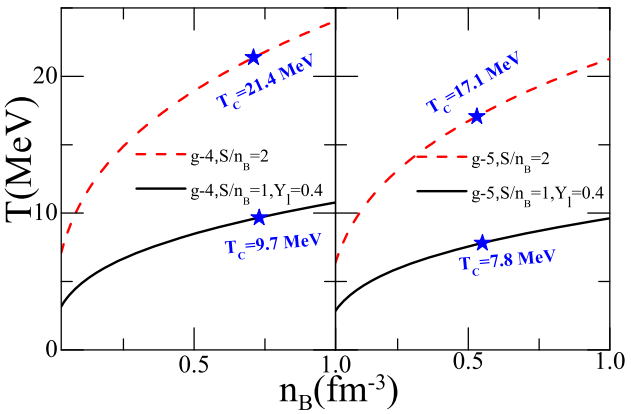

Fig. 7 The core temperature for the star matter as a function of the baryon density

Figure 8 shows the isospin asymmetry of the star matter as a function of the baryon density in the three snapshots along the PQS evolution for g-4 and g-5. From the works [91,109–112], the isospin asymmetry is defined as

$$\delta = 3\frac{n_d - n_u}{n_d + n_u}, \tag{17}$$

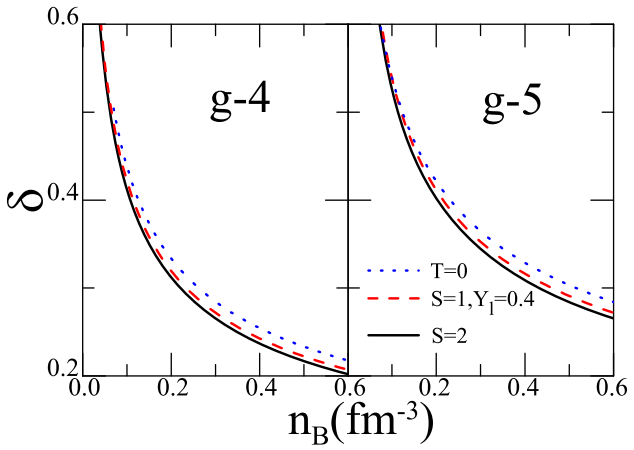

Fig. 8 The isospin asymmetry of the star matter as a function of the baryon density in the three snapshots along the PQS evolution for g-4 and g-5

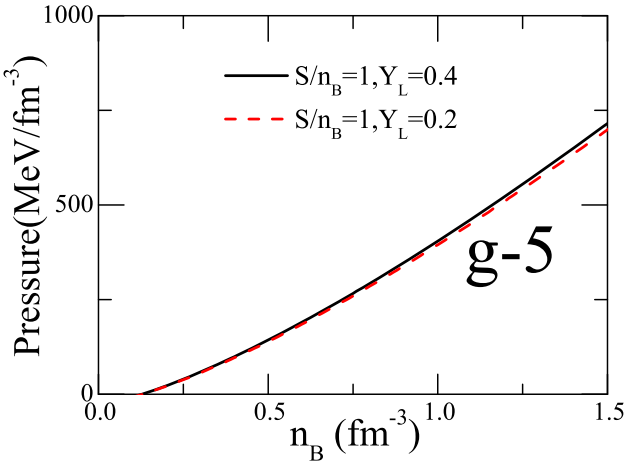

Fig. 9 Pressures as functions of baryon density with different lepton fraction when $S/n_B = 1$ for g-5

which equals to $-n_3/n_B$ with the isospin density $n_3 = n_u - n_d$ and $n_B = (n_u + n_d)/3$ for two-flavor u-d quark matter. One can find in Fig. 8 that the isospin asymmetry δ decreases with the increment of the baryon density inside the stars. Furthermore, one can also see that the isospin asymmetry δ for $T = 0$ stage is larger than those for $S/n_B = 1$, $Y_l = 0.4$ and $S/n_B = 2$ cases. Additionally, the isospin asymmetry δ reaches the smallest value at $S/n_B = 2$ stage (the core temperature of PQSs in this stage is the largest of all the three stages along the star evolution line), and the results above are self-consistent with the conclusion that the difference among u, d, and s quark fraction decreases with temperature in Fig. 3. Combining Figs. 3 and 8, one can also obtain that the difference of the u and d quark fraction and the isospin asymmetry δ both increase with the coupling constant g at a fixed temperature, which indicates that the coupling constant g is closely related to the isospin properties inside the isospin asymmetric quark matter.

In Fig. 9, we calculate the pressures of SQM as functions of baryon density with different lepton fraction $Y_L = 0.4$ and $Y_L = 0.2$ when $S/n_B = 1$ for g-5 in order to find the effects of the fixed lepton fraction in the star matter. One can find in Fig. 9 that the pressure for $Y_L = 0.4$ case is a little larger than that for $Y_L = 0.2$ case at a fixed baryon density for $g - 5$, which indicates that the EOS of star matter can be stiffer with the increasing lepton fraction inside the PQSs. Larger lepton fraction can increase the number of u quark under β-equilibrium condition from star matter, which might be the reason to make the EOS be stiffer, and this phenomenon can also be found when S/n_B is fixed as other values. Furthermore, we also calculate the star mass and the tidal deformability $\Lambda_{1.4}$ with $Y_L = 0.4$ and $Y_L = 0.2$, and the results shows that the maximum mass of the PQS for $Y_L = 0.2$ and $S/n_B = 1$ is 2.62 solar mass, which is less than the maximum mass in $Y_L = 0.4$ and $S/n_B = 1$ case because the EOS from $Y_L = 0.2$ case is softer. For the tidal deformability $\Lambda_{1.4}$ of the PQS for $Y_L = 0.2$ and $S/n_B = 1$, the value is calculated as $\Lambda_{1.4} = 2369$, which is also less than the case of $Y_L = 0.4$ and $S/n_B = 1$. And then we can obtain that both the maximum mass and the tidal deformability $\Lambda_{1.4}$ of the PQS increase with the increment of the lepton fraction inside the star matter.

4 Conclusions

In this work, we have studied the properties of SQM and PQSs within the quasiparticle model. The EOS of SQM has been explored, and we found that the minimum value of the free energy per baryon/energy per baryon decreases/increases with the increment of the temperature or the coupling constant g, and the EOS of SQM can also be stiffen by temperature or the coupling constant g. We have also found that the difference of the quark fractions decreases when the temperature increasing, which would cause the isospin asymmetry of the star matter decreasing at high temperature cases.

Considering the absolutely stable condition for SQM, we have chosen reasonable sets of parameters and further studied the maximum mass of QSs and PQSs along the star evolution line. The recent discovered large mass compact stars PSR J0348+ 0432, MSR J0740+6620, PSR J2215+5135, and especially the GW190814's secondary component m_2 can be well described as QSs within quasiparticle model. Considering three snapshots along the evolution line of PQSs, we have found that the star mass of PQS is larger at the heating stages, which indicates that the heating process in the evolution will increase the maximum mass of PQS.

Moreover, we have also calculated the tidal deformability of QSs and PQSs, and we have found that the tidal deforma-

bility of the larger stars can strongly violates the constraint $\Lambda_{1.4} < 800$ derived from GW170817. Furthermore, we have obtained that the tidal deformability $\Lambda_{1.4}$ for PQSs is larger in the heating stages, and the core temperature of PQSs increases with the entropy per baryon at the heating stages along the star evolution line. We have also found that both the maximum mass and the tidal deformability $\Lambda_{1.4}$ of the PQS increase with the increment of the lepton fraction inside the star matter.

Therefore, our results indicates that considering the effects of temperature within quasiparticle model can significantly influence the properties of the EOS of SQM, fractions of quarks, the entropy of the quark matter, and the tidal deformability and the maximum mass of PQSs along the star evolution line.

Acknowledgements This work is supported by the NSFC under Grants no. 11975132, 11905302, 11505100, 11804179 and 61772295, and the Shandong Provincial Natural Science Foundation, China ZR2019YQ01, ZR2016DB01, ZR2019PA018, ZR2015AQ007, and 2017GSF216010.

Data Availability Statement This manuscript has no associated data or the data will not be deposited. [Authors' comment: This is a theoretical study and no experimental data has been listed.]

Funded by SCOAP[3].

References

1. N.K. Glendenning, *Compact Stars*, 2nd edn. (Spinger-Verlag New York, Inc., New York, 2000)
2. F. Weber, *Pulsars as Astrophyical Laboratories for Nuclear and Particle Physics* (IOP Publishing Ltd, London, 1999)
3. J.M. Lattimer, M. Prakash, Science **304**, 536 (2004)
4. A.W. Steiner, M. Prakash, J.M. Lattimer, P.J. Ellis, Phys. Rep. **410**, 325 (2005)
5. D. Ivanenko, D.F. Kurdgelaidze, Lett. Nuovo Cimento **2**, 13 (1969)
6. N. Itoh, Prog. Theor. Phys. **44**, 291 (1970)
7. A.R. Bodmer, Phys. Rev. D **4**, 1601 (1971)
8. E. Witten, Phys. Rev. D **30**, 272 (1984)
9. E. Farhi, R.L. Jaffe, Phys. Rev. D **30**, 2379 (1984)
10. C. Alcock, E. Farhi, A. Olinto, Astrophys. J. **310**, 261 (1986)
11. F. Weber, Prog. Part. Nucl. Phys. **54**, 193 (2005)
12. I. Bombaci, I. Parenti, I. Vidana, Astrophys. J. **614**, 314 (2004)
13. J. Staff, R. Ouyed, M. Bagchi, Astrophys. J. **667**, 340 (2007)
14. M. Herzog, F.K. Röpke, Phys. Rev. D **84**, 083002 (2011)
15. M.A. Stephanov, K. Rajagopal, E.V. Shuryak, Phys. Rev. Lett. **81**, 4816 (1998)
16. H. Terazawa, INS-Report 336, University of Tokyo (1979)
17. M. Prakash, I. Bombaci, M. Prakash, P.J. Ellis, J.M. Lattimer, R. Knorren, Phys. Rep. **280**, 1 (1997)
18. V.K. Gupta, A. Gupta, S. Singh, J.D. Anand, Int. J. Mod. Phys. D **12**, 583–595 (2003)
19. J. Shen, Y. Zhang, B. Wang, R.-K. Su, Int. J. Mod. Phys. A **20**, 7547–7566 (2005)
20. V. Dexheimer, J.R. Torres, D.P. Menezes, Eur. Phys. J. C **73**, 2569 (2013)
21. V. Dexheimer, D.P. Menezes, M. Strickland, J. Phys. G Nucl. Part. Phys. **41**, 015203 (2014)
22. A. Drago, A. Lavagno, G. Pagliara, Phys. Rev. D **89**, 043014 (2014)
23. A. Drago, G. Pagliara, Eur. Phys. J. A **52**, 41 (2016)
24. A. Bauswein, N. Stergioulas, H. Janka, Eur. Phys. J. A **52**, 56 (2016)
25. J. Antoniadis et al., Science **340**, 6131 (2013)
26. M. Linares, T. Shahbaz, J. Casares, APJ **859**, 54 (2018)
27. H. T. Cromartie et al., Nat. Astron. Lett. **4**, 72 (2020)
28. M. Alford, S. Reddy, Phys. Rev. D **67**, 074024 (2003)
29. M. Alford, P. Jotwani, C. Kouvaris, J. Kundu, K. Rajagopal, Phys. Rev. D **71**, 114011 (2005)
30. M. Baldo, Phys. Lett. B **562**, 153 (2003)
31. N.D. Ippolito, M. Ruggieri, D.H. Rischke, A. Sedrakian, F. Weber, Phys. Rev. D **77**, 023004 (2008)
32. X.Y. Lai, R.X. Xu, Res. Astron. Astrophys. **11**, 687 (2011)
33. M.G.B. de Avellar, J.E. Horvath, L. Paulucci, Phys. Rev. D **84**, 043004 (2011)
34. L. Bonanno, A. Sedrakian, A&A **539**, A16 (2012)
35. P.C. Chu et al., Phys. Rev. D **94**, 123014 (2016)
36. P.C. Chu et al., Eur. Phys. J. C **77**, 512 (2017)
37. P.C. Chu et al., J. Phys. G Nucl. Part. Phys. **47**, 085201 (2020)
38. R. Abbott et al., Astrophys. J. Lett. **896**, L44 (2020)
39. B.P. Abbott et al., Phys. Rev. Lett. **119**, 161101 (2017)
40. L. Rezzolla, E.R. Most, L.R. Weih, Astrophys. J. Lett. **852**(2), L25 (2018)
41. E.R. Most et al., Phys. Rev. Lett. **120**, 261103 (2018)
42. Y. Zhou, L.-W. Chen, Z. Zhang, Phys. Rev. D **99**, 121301(R) (2019)
43. A. Bauswein, O. Just, H.-T. Janka, N. Stergioulas, Astrophys. J. Lett. **850**, L34 (2017)
44. B. Margalit, B.D. Metzger, Astrophys. J. Lett. **850**, L19 (2017)
45. E. Zhou, X. Zhou, A. Li, Phys. Rev. D **97**, 083015 (2018)
46. F.J. Fattoyev, J. Piekarewicz, C.J. Horowitz, Phys. Rev. Lett. **120**, 172702 (2018)
47. E. Annala, T. Gorda, A. Kurkela, A. Vuorinen, Phys. Rev. Lett. **120**, 172703 (2018)
48. D. Radice, A. Perego, F. Zappa, S. Bernuzzi, Astrophys. J. Lett. **852**, L29 (2018)
49. M. Ruiz, S.L. Shapiro, A. Tsokaros, Phys. Rev. D **97**, 021501(R) (2018)
50. J.-E. Christian, A. Zacchi, J. Schaffner-Bielich, Phys. Rev. D **99**, 023009 (2019)
51. G. Montana, L. Tolos, M. Hanauske, L. Rezzolla, Phys. Rev. D **99**, 103009 (2019)
52. P.C. Chu, L.W. Chen, X. Wang, Phys. Rev. D **90**, 063013 (2014)
53. P.C. Chu et al., Phys. Rev. C **99**, 035802 (2019)
54. P.C. Chu et al., Phys. Rev. D **100**, 103012 (2019)
55. P.C. Chu et al., Eur. Phys. J. C **81**, 93 (2021)
56. N.-B. Zhang, B.-A. Li, ApJ **879**, 99 (2019)
57. R. Nandi, P. Char, Astrophys. J. **857**, 12 (2018)
58. V. Paschalidis, K. Yagi, D. Alvarez-Castillo, D. B. Blaschke, A. Sedrakian, Phys. Rev. D **97**, 084038 (2018)

59. The LIGO Scientific Collaboration, The Virgo Collaboration, B.P. Abbott et al., Phys. Rev. X **9**, 011001 (2019)
60. B.P. Abbott et al., Phys. Rev. Lett. **121**, 161101 (2018)
61. K. Schertler, C. Greiner, M.H. Thoma, Nucl. Phys. A **616**, 659 (1997)
62. A. Chodos, R.L. Jaffe, K. Ohnson, C.B. Thorn, V.F. Weisskopf, Phys. Rev. D **9**, 3471 (1974)
63. M. Alford, M. Braby, M. Paris, S. Reddy, Astrophy. J. **629**, 969 (2005)
64. J.Y. Chao et al., Phys. Rev. D **88**, 054009 (2013)
65. P.C. Chu et al., Phys. Rev. D **91**, 023003 (2015)
66. P.C. Chu et al., Phys. Rev. D **93**, 094032 (2016)
67. P.C. Chu et al., Phys. Rev. D **96**, 083019 (2017)
68. Z. Zhang et al., Phys. Rev. D **103**(10), 103021 (2021)
69. P. Rehberg, S.P. Klevansky, J. Hüfner, Phys. Rev. C **53**, 410 (1996)
70. M. Hanauske, L.M. Satarov, I.N. Mishustin, H. Stocker, W. Greiner, Phys. Rev. D **64**, 043005 (2001)
71. S.B. Rüster, D.H. Rischke, Phys. Rev. D **69**, 045011 (2004)
72. D.P. Menezes, C. Providencia, D.B. Melrose, J. Phys. G **32**, 1081 (2006)
73. C.D. Roberts, A.G. Williams, Prog. Part. Nucl. Phys. **33**, 477 (1994) and references therein
74. H.S. Zong, L. Chang, F.Y. Hou, W.M. Sun, Y.X. Liu, Phys. Rev. C **71**, 015205 (2005)
75. S.X. Qin, L. Chang, H. Chen, Y.X. Liu, C.D. Roberts, Phys. Rev. Lett. **106**, 172301 (2011)
76. B.A. Freedman, L.D. Mclerran, Phys. Rev. D **16**, 1169 (1977)
77. E.S. Fraga, R.D. Pisarski, J. Schaffner-Bielich, Phys. Rev. D **63**, 121702(R) (2001)
78. E.S. Fraga, P. Romatschke, Phys. Rev. D **71**, 105014 (2005)
79. A. Kurkela, P. Romatschke, A. Vuorinen, Phys. Rev. D **81**, 105021 (2010)
80. G.N. Fowler, S. Raha, R.M. Weiner, Z. Phys. C **9**, 271 (1981)
81. S. Chakrabarty, S. Raha, B. Sinha, Phys. Lett. B **229**, 112 (1989)
82. S. Chakrabarty, Phys. Rev. D **43**, 627 (1991)
83. S. Chakrabarty, Phys. Rev. D **48**, 1409 (1993)
84. S. Chakrabarty, Phys. Rev. D **54**, 1306 (1996)
85. O.G. Benvenuto, G. Lugones, Phys. Rev. D **51**, 1989 (1995)
86. G.X. Peng, H.C. Chiang, J.J. Yang, L. Li, B. Liu, Phys. Rev. C **61**, 015201 (1999)
87. G.X. Peng, H.C. Chiang, B.S. Zou, P.Z. Ning, S.J. Luo, Phys. Rev. C **62**, 025801 (2000)
88. G.X. Peng, A. Li, U. Lombardo, Phys. Rev. C **77**, 065807 (2008)
89. A. Li, G.X. Peng, J.F. Lu, Res. Astron. Astrophys. **11**, 482 (2011)
90. K. Schertler, C. Greiner, P.K. Sahu, M.H. Thoma, Nucl. Phys. A **637**, 451 (1998)
91. P.C. Chu, L.W. Chen, Astrophys. J. **780**, 135 (2014)
92. P.C. Chu et al., Phys. Lett. B **778**, 447 (2018)
93. P.C. Chu, L.W. Chen, Phys. Rev. D **96**, 103001 (2017)
94. R.D. Pisarski, Nucl. Phys. A **498**, 423 (1989)
95. X.J. Wen et al., J. Phys. G Nucl. Part. Phys. **36**, 025011 (2009)
96. X.J. Wen et al., Phys. Rev. D **86**, 034006 (2012)
97. B.K. Patra, C.P. Singh, Phys. Rev. D **54**, 3551 (1996)
98. J.R. Oppenheimer, G.M. Volkoff, Phys. Rev. **33**, 374 (1939)
99. A.W. Steiner, M. Prakash, J.M. Lattimer, Phys. Lett. B **509**, 10 (2001)
100. A.W. Steiner, M. Prakash, J.M. Lattimer, Phys. Lett. B **486**, 239 (2000)
101. S. Reddy, M. Praskash, J.M. Lattimer, Phys. Rev. D **58**, 013009 (1998)
102. D.P. Menezes, A. Deppman, E. Megias, L.B. Castro, arXiv:1410.2264v2
103. G.Y. Shao, Phys. Lett. B **704**, 343 (2011)
104. T.E. Riley et al., Astrophys. J. Lett. **887**, L21 (2019)
105. M.C. Miller et al., Astrophys. J. Lett. **887**, L24 (2019)
106. S. Postnikov, M. Praskash, J.M. Lattimer, Phys. Rev. D **82**, 024016 (2010)
107. J. Xu, L.-W. Chen, B.-A. Li, Phys. Rev. C **91**, 014611 (2015)
108. Z. Cao et al. (2020). arXiv:2009.00942
109. M. Di Toro, A. Drago, T. Gaitanos, V. Greco, A. Lavagno, Nucl. Phys. A **775**, 102 (2006)
110. G. Pagliara, J. Schaffner-Bielich, Phys. Rev. D **81**, 094024 (2010)
111. M. Di Toro, V. Baran, M. Colonna, V. Greco, J. Phys. G **37**, 083101 (2010)
112. G.Y. Shao, M. Colonna, M. Di Toro, B. Liu, F. Matera, Phys. Rev. D **85**, 114017 (2012)